EAI Endorsed Transactions
on Sustainable Manufacturing and Renewable Energy Research Article EAI.EU

Experimental test to analyze and evaluate the exergy and energy efficiency of the AHU in the Waterchiller system

Van Cuong Bui[1], Duc Khuyen Nguyen[1], Thanh Nhan Phan[2,3,*]

[1] Faculty of Engineering and Technology, Nong Lam University, Quarter 33, Linh Trung Ward, Ho Chi Minh City, Vietnam
[2] Department of Heat and Refrigeration, Faculty of Mechanical Engineering, Ho Chi Minh City University of Technology (HCMUT), 268 Ly Thuong Kiet Street, District 10, Ho Chi Minh City, Vietnam
[3] Vietnam National University Ho Chi Minh City, Linh Trung Ward, Ho Chi Minh City, Vietnam

Abstract

Experimental study to determine the impact of changing AHU operating parameters on exergy and energy efficiency in the water chiller system. The study used both an experimental method and theoretical calculations, with a Trane-brand chiller system with a cooling capacity of 25,3 kW. The results showed that when the supply air temperature increased from 295 K to 299 K, the heat exchanger's exergy consumption ($X_{cons,HE}$) decreased from 0.2 kW to about 0.05 kW. The exergy consumption of the heat exchanger ($X_{cons,HE}$) and the exergy flow of the return air to the AHU ($X_{a,re}$) were almost constant, maintained at about 0.95 kW and 0.8 kW, showing that the efficiency of the heat exchanger and the exergy of the ambient air were relatively stable, not much affected by changes in ambient temperature. When the inlet water temperature ($X_{w,in}$) increases from 284 K to 289 K. The water exergy flow (X_w) decreases linearly from about 1.3 kW to about 0.8 kW. In addition, this study also evaluates the impact of changing the chilled water pump frequency and air flow rate on energy efficiency. The results indicate that the optimal operating point is not at the maximum frequency but at about 45 Hz, at which the cooling capacity reaches 7,764 kW.

Keywords: Water chiller, Performance, Energy consumption, Exergy, Heat transfer.

Received on 01 December 2025, accepted on 17 December 2025, published on 22 December 2025

doi: 10.4108/eetsmre.11169

*Corresponding author: phannhan@hcmut.edu.vn

1. Introduction

Vietnam has a hot, humid tropical climate, so air conditioning plays a crucial role in daily life and industry. Along with population and economic growth, demand for air conditioners is increasing, particularly in high-rise buildings used as commercial centers and offices. The COP26 conference has reached an agreement to limit the Earth's temperature rise to less than 1.5 degrees Celsius over the next decade, reducing greenhouse gas emissions and moving towards the goal of Net-Zero Carbon Emissions. At the conference, the Vietnamese representative, Prime Minister Pham Minh Chinh, delivered a speech and committed to achieving net-zero emissions by 2050. Following Vietnam's commitment at COP26, the country has taken steps to implement measures across all industries to reduce greenhouse gas emissions. Consequently, energy has become a top-priority macro issue.

Tzong-Shing Lee and Wan-Chen Lu [1] compared and evaluated the efficiency of 6 chiller models for predicting the energy efficiency of water chillers using steam compression. These models are often used to optimize system operations and minimize energy consumption. This research provides a crucial foundation for the development and refinement of subsequent research models, ultimately enhancing energy efficiency in the HVAC sector. Additionally, the study by R. Saidur et al. [2] analyzes energy consumption, energy savings, and emissions from chillers in buildings. Refrigeration systems play a crucial role in maintaining comfortable indoor environmental conditions, but they are also among the largest energy consumers. Therefore, the optimal assessment of the refrigeration system, in general, and the chiller, in particular, helps us control energy losses. The results of the study by F.W. Yu and K.T. Chan [3] show that load-based cooling tower fan and condensate pump speeds can significantly reduce energy consumption compared to systems using fixed-speed fans and pumps. Additionally, this study demonstrates that applying an optimal control method, combined with variable condensate flow, can reduce the chiller system's power consumption and annual operating costs. N. Trautman et al. [4] have optimized operating parameters, such as pumping speed and chilled water temperature, to identify an optimal operating model with high potential to improve energy efficiency and reduce operating costs in buildings. Hang Yin et al. [5] demonstrated that exergy analysis provides greater insight and detail into a system's energy efficiency than traditional analytical methods. A.Yildiz & Mustafa A.E. [6] analyzed the energy and exergy of the absorption diffusion refrigeration system, thereby evaluating the thermodynamic performance of the system. Exergy analysis aims to identify sources of energy loss, thereby pinpointing factors that affect energy efficiency and the potential for energy savings, while also minimizing environmental impacts. An approach developed by T. Morosuk & G. Tsatsaronis [7] provides significant insight into the performance of absorption refrigeration systems, thereby improving understanding of the source of energy loss (exergy loss). Jia Yang et al. [8] demonstrated that controlling the condensation temperature with an optimal dew rate can increase the coefficient of performance (COP) by up to 51.5% and significantly reduce power consumption. Zhimin Du et al. [9] introduce the exergy analysis method and the Perfect Control Index (PCI) to evaluate HVAC control strategies for airport HVAC systems. This indicates that even the optimal strategy can improve significantly beyond the ideal operating level. M. A. Ehyaei et al. [10] comprehensively analyzed the performance, economy, and environmental impact (3E) of using an absorption chiller to cool the gas inlet of a gas turbine. The results show that the technology is economical and significantly increases the output power, while improving cycle performance in hot climates. F. Panahizadeh et al [11] conducted in-depth research on the 4E analysis (energy, exergy, economy, optimization) for single-stage absorption chiller networks. The authors employed a multi-objective optimization algorithm (MOPSO) to determine operating conditions that maximize ECOP and minimize annual operating costs. F.W. Yu et al [12] reviewed national standards and guidelines for the energy efficiency of commercial refrigeration systems. Yuying Sun et al. [13] developed a method to maintain a comfortable temperature environment and achieve significant energy savings (11.0%) compared to traditional fixed-control methods. In Suamir et al. [14], the proposed solution is to adopt a variable-speed pumping system and a balancing valve (two-way valve) to improve the chiller's temperature performance and energy efficiency. W.T.Ho & F.W.Yu [15] used the L-FGS-B optimization algorithm, demonstrating the potential to reduce annual power consumption by 9.14%-16.67% through optimal operational control strategies.

The above studies demonstrate that calculating exergy to conserve energy in refrigeration systems has attracted significant attention from researchers. Therefore, this paper focuses on empirical research evaluating changes in input parameters affecting energy efficiency, as well as how changes in pumping frequency affect the energy efficiency of the AHU system.

2. Literature review

The assumed system is shown in Figure 1. For simplicity, it was assumed that there is only one AHU (Air Handling Unit) on the demand side and one pump for supplying the chilled water.

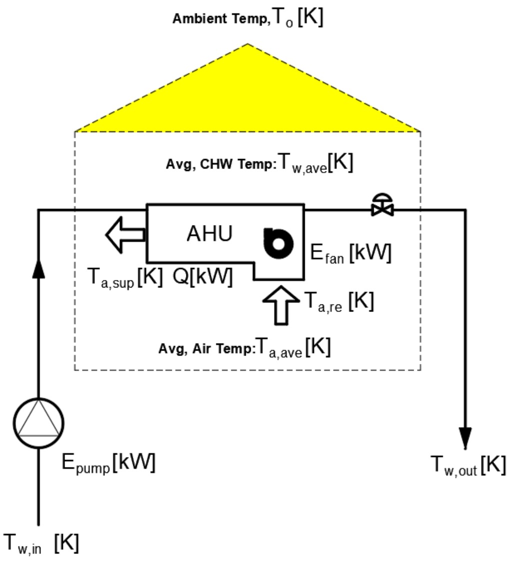

Fig.1 Assumed chilled water circuit in AHU

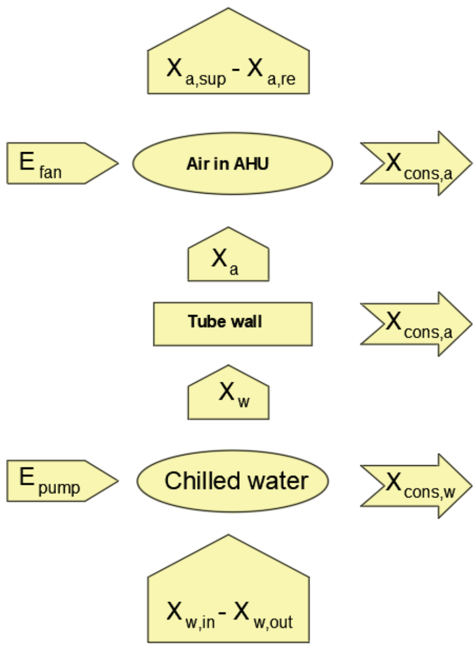

Fig.2 Flow of exergy through the AHU

Budgetary consumption of energy and exergy for an air conditioning system. [5]

$$E_{fan} + \frac{c_a\rho_a F_a(T_{a,re}-T_o)}{3600} = \frac{c_a\rho_a F_a(T_{a,sup}-T_o)}{3600} + Q \quad (1);$$

$$\frac{c_a\rho_a F_a \ln(T_{a,re}/T_o)}{3600} + S_{g,a} = \frac{c_a\rho_a F_a \ln(T_{a,sup}/T_o)}{3600} + Q/T_{a,ave} \quad (2);$$

From (1) and (2) to ambient temperature, to [K], the energy consumption budget of exergy is developed

$$E_{fan} + X_a - X_{cons,a} = X_{a,\text{sup}} - X_{a,re} \quad (3);$$

The flow of exergy through the three subsystems is shown in Figure 2.

According to (4) and (5) at the T_o Temperature, we can calculate the exergy budget of the pipe wall system (6), from (7) and (8) at the T_o At a given temperature, we find the exergy budget of the Waterchiller system (9).

$$Q_a = Q_w \quad (4); \quad \frac{Q}{T_{a,ave}} + S_{g,HE} = \frac{Q}{T_{w,ave}} \quad (5);$$

$$X_w - X_{cons,HE} = X_a \quad (6);$$

$$E_{\text{pump}} + \frac{c_w\rho_w F_w(T_{w,in}/T_o)}{3600} + Q = \frac{c_w\rho_w F_w(T_{w,out}/T_o)}{3600} \quad (7);$$

$$\frac{c_w\rho_w F_w \ln(T_{w,in}/T_o)}{3600} + \frac{Q}{T_{a,ave}} + S_{g,w} = \frac{c_w\rho_w F_w \ln(T_{w,out}/T_o)}{3600} \quad (8);$$

$$E_{\text{pump}} + X_{w,in} - X_{cons,a} = X_w - X_{w,\text{out}} \quad (9);$$

The exergy budget for the entire system is determined by

$$[(E_{\text{pump}} + E_{\text{fan}}) + (X_{w,\text{in}} + X_{w,\text{out}})] - (X_{\text{cons},a} + X_{\text{cons},HE} + X_{\text{cons},w}) = X_{a,\text{sup}} - X_{a,re} \quad (10);$$

The net exergy input rate from the chiller to the chilled water circuit is determined by

$$X_{w,\text{in}} = \frac{c_w\rho_w F_w(T_{w,\text{in}}-T_o)}{3600} - \frac{c_w\rho_w F_w T_o \ln(T_{w,\text{in}}/T_o)}{3600} \quad (11);$$

$$X_{w,\text{out}} = \frac{c_w\rho_w F_w(T_{w,\text{out}}-T_o)}{3600} - \frac{c_w\rho_w F_w T_o \ln(T_{w,\text{out}}/T_o)}{3600} \quad (12);$$

Exergy consumed in the air channel inside the AHU, in the tube wall between air and water, and in the water inside the cold-water vein are determined by (13), (14), and (15), respectively.

$$X_{cons,a} = S_{g,a}T_o \quad (13);$$

$$X_{\text{cons},HE} = S_{g,HE}T_o \quad (14);$$

$$X_{cons,w} = S_{g,w}T_o \quad (15);$$

The output exergy power ratio is the ratio of the net output exergy power from the AHU to the indoor space to the exergy power ratio due to the return air flow entering the AHU, as given by (16) and (17), respectively.

$$X_{a,\,\text{sup}} = \frac{c_a\rho_a F_a(T_{a,\,\text{sup}} - T_o)}{3600} - \frac{c_a\rho_a F_a T_o \ln\,(T_{a,\,\text{sup}} - T_o)}{3600} \quad (16);$$

$$X_{a,re} = \frac{c_a\rho_a F_a(T_{a,re} - T_o)}{3600} - \frac{c_a\rho_a F_a T_o \ln\,(T_{a,re} - T_o)}{3600} \quad (17);$$

The ratio of exergy power due to the absorption airflow due to heat release, and the ratio of exergy power discharged from cold water due to heat absorption are determined by (18) and (19)

$$X_a = \left(1 - \frac{T_o}{T_{a,\text{ave}}}\right)(-Q) \quad (18); \quad X_w = \left(1 - \frac{T_o}{T_{w,\text{ave}}}\right)(-Q) \quad (19);$$

In those equations, T_{ave} [K] is the average air temperature, $T_{w,ave}$ [K] is the average cold water temperature in the AHU, $T_{a,sup}$ [K] và $T_{a,re}$ [K] is approximated by the mean assumptions of the supply and return air temperatures, $T_{w,in}$ [K] and $T_{w,out}$ [K] is the inlet and outlet temperatures of the cold water circuit, c_a [kJ/kgK], c_w [kJ/kgK], ρ_a [kg/m^3], ρ_w [kg/m^3], F_a [m^3/h], F_w [m^3/h] Specific heat capacity, density and flow of air and cold water, respectively. Q [kW] is the heat energy exchanged in the AHU. $S_{g,a}$ [kW/K], $S_{g,HE}$ [kW/K], $S_{g,w}$ [kW/K] is the rate at which entropy is generated in the air inside the AHU, in the tube wall between air and water, and in the water inside the cold-water vein, respectively.

3. Experiment Design

3.1 Design of Experiments Methods

The air-cooling water chiller system model CGAT085, as shown in Figure 3, with a refrigeration capacity of 25,3 kW, using R407C refrigerant and a power supply of 380 – 450/3/50 manufactured by Trane, installed at building B5 of Ho Chi Minh City University of Technology, VNU–HCM. The compressor is a closed spiral type with a plate evaporator, a wing-tube condenser, and a thermal throttle valve. The condenser fan is axial, with an airflow of 5768 cfm and a motor power of 320 W. The entire system has dimensions of 1050×950×1080 mm and a weight of 204 kg, which basically meets the standards for conducting experiments.

Fig.3 Water chiller system model

Table 1.
Measuring instruments

Device	Model	Error
Wind Speed Gauge	Testo	± 0,1 m/s
Temperature Gauge	Dataloger Extech SDL200	± 0.1 ºC
Flow Meter	Airflow TSI EBT721	± 0,3 %
Temperature and Humidity Recorder	LaserLinear	± 0,3 %

Sample size and data collection method: Each test case is performed over different temperature ranges, and data is collected at 10 points to ensure accuracy.

3.2 Statistical Design of Experiment

The ambient temperature and return air temperature were assumed to be constant at 310K and 303K, respectively. The supply air and supply water temperatures were set to 295K and 285K, respectively. The return water temperature was assumed to be 278K higher than the supply water temperature under full-load conditions. Still, it can vary with the AHU heat-transfer rate and the variable-flow control method under partial-load conditions. The flow rate, pumping head, and pump power at full load were assumed to be 3.93 m^3/h, 20 m, and 0.75 kW, respectively. The fan power at full load was assumed to be 1.085 kW. The respective quadratic curves characterized both the system and the pump performance. For TV control, when the flow rate was zero, the pumping head was assumed to be 1.4 times the rated pumping head. The pumping head, based on a constant pressure difference in CDP control, was assumed to be 10 m.

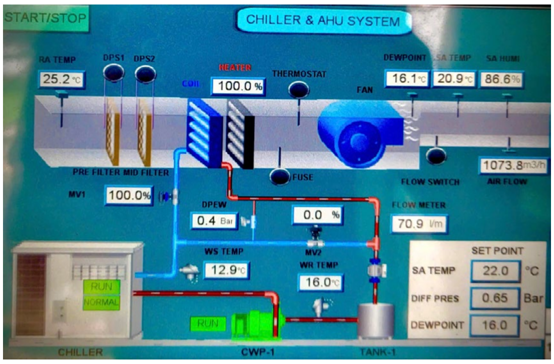

Fig.4 Waterchiller system principal diagram

4. Results analysis and Discussion

4.1 Exergy analysis throughout AHU equipment

4.1.1 Effect of supply air temperature

The exergy rate at full load (21 kW) with supply air temperatures of 295 - 299K is shown in Figure 5.

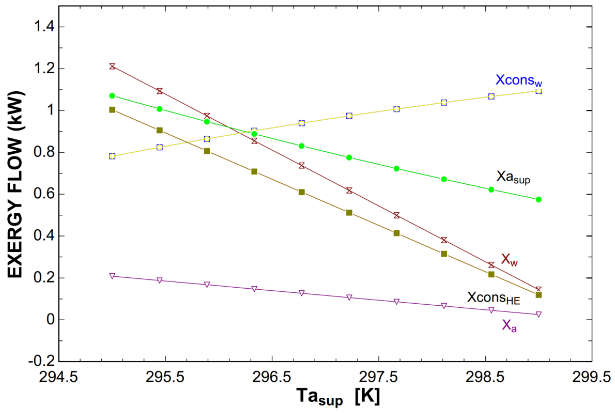

Fig.5 Variation of exergy at the supply air condition

This diagram depicts the variation of exergy currents in a thermal system, which is affected by the supply air temperature ($T_{a,sup}$). The analysis shows that the system's overall performance is closely related to environmental conditions. When the supply air temperature increases from 295 K to 299 K, the main exergy currents of the system tend to decrease. Specifically, the exergy flow of water (X_w) dropped the most, from about 1.2 kW to only 0.15 kW, indicating that the role of water in the supply of sound energy was significantly reduced. Similarly, the exergy flow of the air feed ($X_{a,sup}$) also decreased from 1.05 kW to 0.6 kW, indicating that the exergy efficiency of the air decreases with ambient temperature. However, the consumption of exergy in water and in cold water geysers ($X_{cons,\mathrm{w}}$) increased from 0.8 kW to 1.08 kW as the ambient temperature increased. This inconsistency indicates a significant exergy loss in the process, especially at high temperatures. Besides, a positive point is the exergy consumption of the heat exchanger ($X_{cons,\mathrm{HE}}$) decreased from 0.2 kW to about 0.05 kW. This suggests that the heat exchanger performs more efficiently at higher temperatures, although overall system-wide losses continue to increase.

4.1.2 Effect of ambient temperature

The exergy rate at full load with ambient temperatures from 307K to 313K is shown in Figure 6.

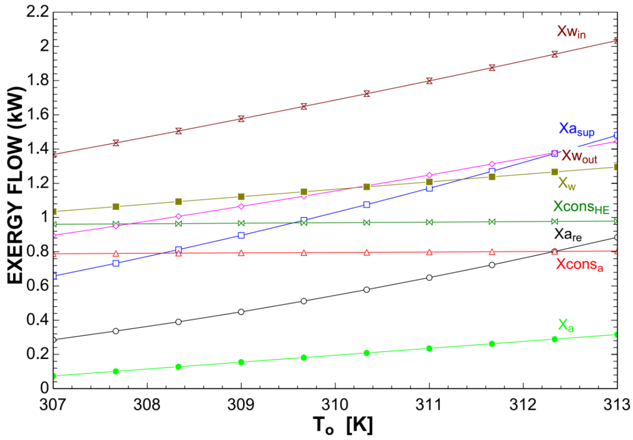

Fig.6 Variation of exergy of AHU at ambient temperature

The figure showed a significant increase in water inlet exergy flow ($X_{w,\,\mathrm{in}}$), increase linearly from about 1.4 kW to almost 2.0 kW as the ambient temperature rises from 307K to 313K. This indicates that the system needs to provide more useful energy from the water source as the ambient temperature increases. In contrast, the exergy flow of the inlet air ($X_{a,sup}$) and the exergy flow of the output water ($X_{w,\,\mathrm{out}}$) tended to increase slightly but insignificantly, from 0.65 kW to about 1.4 kW and from 0.75 kW to about 1.4 kW, respectively. The lines represent the exergy consumption of air and AHU ($X_{cons,a}$) and of water (X_w) showing a steady uptrend. Concrete, $X_{cons,a}$ increased from about 0.3 kW to nearly 0.8 kW, indicating that the functional energy loss during air treatment rises significantly when the ambient temperature is higher. Finally, the exergy line consumes the heat exchanger ($X_{cons,\mathrm{HE}}$) and the exergy flow of return air to the AHU ($X_{a,re}$) almost unchanged, maintained at about 0.95 kW and 0.8 kW, showing that the efficiency of the heat exchanger and the exergy of the ambient air are relatively stable, not much affected by the change of ambient temperature.

4.1.3 Effect of inlet water temperature

The differences in the exergy rate are shown in Figure 7 for the inlet water temperatures of AHU (284K and 289K).

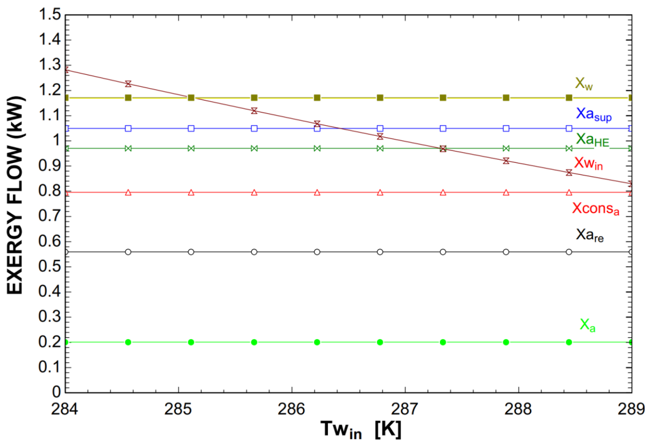

Fig.7 Variation of exergy at inlet water temperature

The chart depicts the change of lines exergy when the inlet water temperature ($T_{w,\,\mathrm{in}}$) increased from 284K to 289K. Overall, the graph shows a fairly straightforward linear relationship between water temperature and some exergy currents, while others remain almost unchanged. Exergy flow of water (X_w) the linear reduction from about 1.3 kW to about 0.8 kW is because, as the input water temperature increases, the temperature difference between the water and the environment decreases, reducing the sound energy the system can extract from the water. In addition, the exergy flow of the air supply ($X_{a,sup}$) and exergy series of heat exchangers ($X_{cons,\mathrm{HE}}$) almost unchanged, at about 1.1 kW and 0.95 kW, respectively. Exergy flow of outlet air (X_a) and exergy flow of air return ($X_{a,re}$) also remained stable, at about 0.2 kW and 0.55 kW, respectively. This stability shows that the system's performance in terms of air is not significantly affected by changes in inlet water temperature.

4.2 Evaluation of the effects of changing chilled water pump frequency and air flow on energy efficiency

We let the chiller system run to steady state, then start recording the values displayed on the control panel and the gauges. We then increase the frequency and airflow through the AHU linearly. We continue to wait until the system reaches a stable state, then record the data. The traffic value milestones we will record at the levels of 1000 m^3/h, 1200 m^3/h, 1400m^3/h, 1600 m^3/h, 1800 m^3/h and the lowest high is 2000 m^3/h (ignoring the case of fresh air supply). Correspondingly, we will calculate the case of the pumping frequency at 30 Hz, 35 Hz, 40 Hz, 45 Hz, 50 Hz.

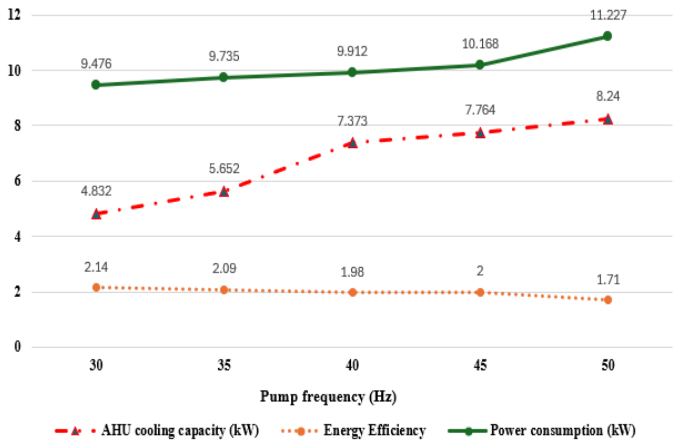

Fig.8 The influence of pumping frequency

This diagram illustrates the relationship between pumping frequency and refrigeration system efficiency, highlighting clear trends to be considered in operational optimization. As the pumping frequency increases from 30 Hz to 50 Hz, both AHU cold yield and system cold power increase steadily, from 4.83 kW to 8.24 kW and from 19.78 kW to 24.07 kW, respectively. However, the power consumption also increased from 9,476 kW to 11,227 kW in the same frequency range. Although the rate of increase in electricity consumption was relatively slow, overall energy efficiency declined from a peak of 2.14 at 30 Hz to a low of 1.71 at 50 Hz. This decline in efficiency warns that, although the system can accommodate greater cold loads, the cost of electricity per refrigeration unit has increased. Therefore, the optimal operating point is not at the maximum frequency but rather around 45 Hz, where the cold productivity reaches 7,764 kW. At the same time, the energy efficiency remains at 2.0, providing the best economic-technical balance.

5. Conclusion

In this study, an exergy analysis of an assumed chilled-water circuit with five variable-flow control modes was conducted. Subsequently, the exergy budget of an actual chilled water circuit. The variable-frequency transformation of the chilled water pump was compared. The calculations indicate that variable-frequency control and a higher chilled water temperature can effectively reduce the exergy consumption rate and improve exergy efficiency.

In addition, the airflow through the AHU is regulated by an inverter, improving cooling efficiency and reducing energy consumption. Still, if it is reduced excessively, it can affect the quality of the room's microclimate. Therefore, the optimal solution is to flexibly combine taking advantage of condensate from the indoor unit with adjusting the pump frequency and airflow using an intelligent control system. This approach both ensures energy efficiency and maintains user comfort, thereby optimizing the operation of the air-cooling chiller system.

Acknowledgements.

We acknowledge Ho Chi Minh City University of Technology (HCMUT), VNU-HCM for supporting this study.

References

[1] Tzong-Shing Lee, W.-C.L. (2010). An evaluation of empirically-based models for predicting energy performance of vapor-compression water chillers. Applied *Energy*,. **87**.

[2] Saidur, R.H., M. Mahlia, T. M. I., and N.A. Rahim, Mohammed H. A. (2011). *Chillers energy consumption, energy savings, and emission analysis in institutional buildings. Energy*, **36**(8): p. 5233–5238.

[3] F.W. Yu, K.T.C.(2008). Optimization of water-cooled chiller system with load-based speed control. *APPLIED ENERGY*, **85**: p. 931–950.

[4] Neal Trautman, A.R., Jie Chen, (2021). Overall chilled water system energy consumption modeling and optimization. *Applied Energy*, **299**.

[5] Hang Yin, R.O., Masanori Shukuya, (2015). Application of Exergy Analysis to Chilled Water Circuit and Heat Pump System. *Energy Procedia,* **78**: p. 1075–1080.

[6] Abdullah Yıldız, M.A.E., (2013). Energy and exergy analyses of the diffusion absorption refrigeration system. *Energy*, p. 1–9.

[7] Tatiana Morosuka, G.T., (2008). A new approach to the exergy analysis of absorption refrigeration machines. *Energy*, **33**: p. 890–907.

[8] Jia Yang, K.T.C., Xiangsheng Wu, F.W. Yu, Xiaofeng Yang, (2012). An analysis on the energy efficiency of air-cooled chillers with water mist system. *Energy and Buildings*, **55**: p. 273–284.

[9] Zhimin Du, X.J., BoFan, (2015). Evaluation of operation and control in HVAC (heating, ventilation, and air conditioning) system using exergy analysis method. *Energy*, p. 1–10.

[10] M. A. Ehyaei, S.H., N. Enadi and P. Ahmadi, (2011). Exergy, economic and environment (3E) analysis of absorption chiller inlet air cooler used in gas turbine power plants. *INTERNATIONAL JOURNAL OF ENERGY RESEARCH,* **36**: p. 486–498.

[11] F. Panahizadeh, M.H., M. Farzaneh-Gord, A. A. V. Ochoa, (2020). Energy, exergy, economic analysis and optimization of single-effect absorption chiller network. *Journal of Thermal Analysis and Calorimetry,*

[12] F.W. Yua, K.T.C., R.K.Y. Sitc and J. Yang, (2014). *Review of standards for energy performance of chiller systems serving commercial buildings.* Energy Procedia. **61**: p. 2778 – 2782.

[13] Yuying Sun, H.X., Wei Wang, Shangjiang Wu, Yong Wu, Yang Hong, Shiming Deng, (2020). Development of an optimal control method of chilled water temperature for constant-speed air-cooled water chiller air conditioning systems. *Applied Thermal Engineering*, p. 1–62.

[14] I N Suamir, S., I N Ardita, G Santanu, (2020). Experimental and numerical optimization on chilled water configuration for improving temperature performance and economic viability of a centralized chiller plant. *Journal of Physics*, **1450**.

[15] W.T. Ho, F.W.Y., (2020). Improved model and optimization for the energy performance of chiller system with diverse component staging. *Energy*.